Simulation of an Octupole Scanning Magnet for Spot Scanning in Proton Therapy

Bolei Jia, Lianhua Ouyang, and Zhentang Zhao

***Abstract*—Current proton therapy scanning systems always use two independent dipole magnets for spot scanning in proton therapy. However, the space occupied by these two dipole magnets located after the final gantry bending magnets is very large and increases the overall size of the gantry. In order to construct a compact nozzle and decrease the size of the gantry, we decide to design an octupole scanning magnet to replace these two separate dipole magnets. The octupole scanning magnet, which is completely different from traditional octupole magnet, can generate rotating dipole magnetic field with the change of the loaded sinusoidal current phases. In this paper, we have finished the static optimization of an octupole scanning magnet model, including the length and shape of the poles, the diameter of the gap, and the shims on the pole edges, both in Opera two-dimensional (2-D) and 3-D. The corresponding relationship between the size of the gap and the good field region was also studied. The effect of eddy currents on magnetic field stability was also simulated in Opera 3-D. All the simulation results are presented in this paper.**

***Index Terms*—Spot scanning, gantry, octupole scanning magnet, static optimization, eddy current.**

I. Introduction

THE proton therapy has attracted increasing interest for cancer treatment in recent years. Most scanning systems of the current proton therapy facility always consist of two independent dipole magnets for spot scanning [1]. The scan magnet system is installed in the nozzle located after the final gantry bending magnets. The two independent dipole magnets are required to be arranged one after another for controlling the deflection of the proton beam in the transverse directions [2]. The space occupied by these two scanning magnets directly determines the size of the gantry.

The major problem existing in the design of a gantry is its size [3]. A large gantry always leads to high cost of the proton therapy facility. In order to design a compact nozzle and miniaturize the overall size of the gantry, we plan to replace the two dipole magnets with the scanning octupole magnet proposed by the researchers recently to reduce the space occupied by scanning magnets. The octupole scanning magnet can generate a rotating dipole magnetic field in its bore when each pair of opposing poles is given a regular sinusoidal current provided by four independent power supplies [4]. In addition, the space occupied by the octupole scanning magnet, compared with the current scanning magnets, is significantly reduced. For a further study on the octupole scanning magnet, we designed a model and carried out some simulations to investigate its static field distribution and dynamic processes. The cross section and main dimensions of the octupole scanning magnet model are presented in Fig. 1.

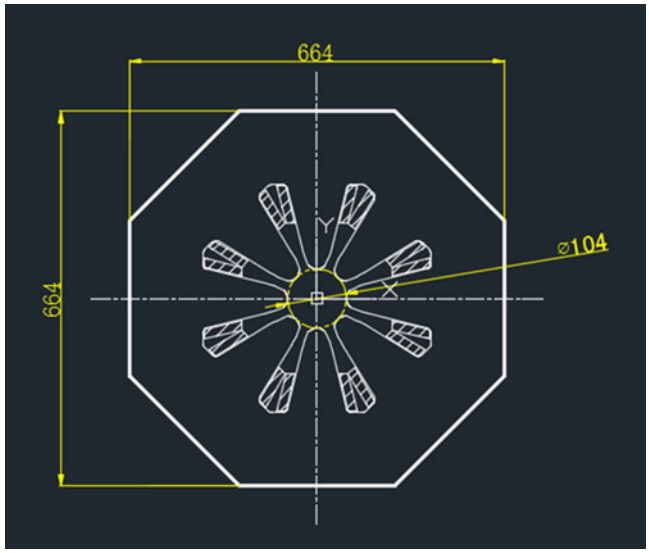

Fig. 1. The cross section of the octupole scanning magnet model.

II. Design Parameters of the Model

We assume that the maximum energy of the proton beam is 235 MeV and the distance from the center of the scanning octupole magnet model to the iso-center is 2.1 m. The diameter of the treatment volume is assumed to be 30 cm. Thus, the octupole scanning magnet should be able to deflect the proton beam by 15 cm at the iso-center. Under these assumptions, we obtain the maximum deflection angle of the proton beam is 71.429 mrad and the value of the integrated field is 0.1679 Tm. We take the mechanical length of the magnet model for 35 cm and get the maximum magnetic field $B_m = 4795$ Gs. Accordingly, the beam exiting from the magnet is 1.25 cm away from

Manuscript received August 29, 2017; accepted October 30, 2017. Date of publication November 15, 2017; date of current version November 30, 2017. *(Corresponding author: Bolei Jia.)*

B. Jia is with the Shanghai institute of Applied Physics, Chinese Academy of Sciences, Shanghai 201800, China, and also with the University of Chinese Academy of Sciences, Beijing 100049, China, and ShanghaiTech University, Shanghai 201210, China (e-mail: jiabolei@sinap.ac.cn).

L. Ouyang and Z. Zhao are with the Shanghai Institute of Applied Physics, Chinese Academy of Sciences, Shanghai 201202, China (e-mail: ouyanglianhua@sinap.ac.cn; zhaozhentang@sinap.ac.cn).

Color versions of one or more of the figures in this paper are available online at http://ieeexplore.ieee.org.

Digital Object Identifier 10.1109/TASC.2017.2773828

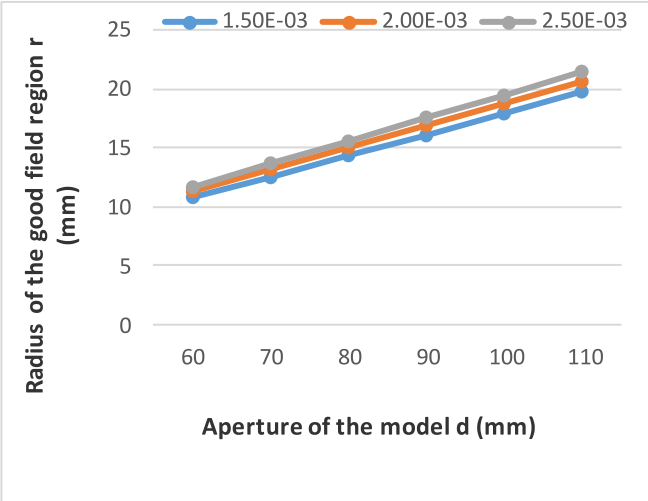

Fig. 2. The relationship between the aperture and the radius of the good field region in different field homogeneity.

TABLE I
MAIN PARAMETERS OF THE SIMULATED MAGNET MODEL

Parameter	Value
Distance away from the iso-center	2.1 m
Integrated field	0.1679 Tm
Mechanical length	35 cm
Good Field Region (Radius)	20 mm
Field homogeneity (ratio)	$\pm 2.5 \times 10^{-3}$
Aperture	102 mm

the central axis of the model. Considering the beam spot size, we finally determined the radius of its good field region as 20 mm. The clinically required beam position error is in the range of ± 0.5 mm at the iso-center [5]. According to the requirement, the magnetic field homogeneity ($\delta = \Delta B/B_0$, B_0 is the field at the center of the magnet.) in its good field region should be in the range of $\pm 2.5 \times 10^{-3}$.

In order to obtain the aperture of the magnet model, we performed some simulations using Opera 2D to investigate the relationship between the good field region and the aperture. We obtained the radius of different good field regions by changing the aperture of the magnet under the same field homogeneity. The simulated results are presented in Fig. 2. It indicates that the radius of the good field region is approximately proportional to the aperture of the octupole scanning magnet and the scale factor dependents on the required field homogeneity. With the required $\pm 2.5 \times 10^{-3}$ field homogeneity and the size of the good field region, we finally determined the aperture to 104 mm. The main parameters of the magnet model are listed in Table I.

III. STATIC SIMULATIONS

A. 2D Static Optimization

Magnetic saturation can deteriorate the field quality in the aperture of the model. In order to avoid serious magnetic saturation on the pole, special attention was given to the optimization

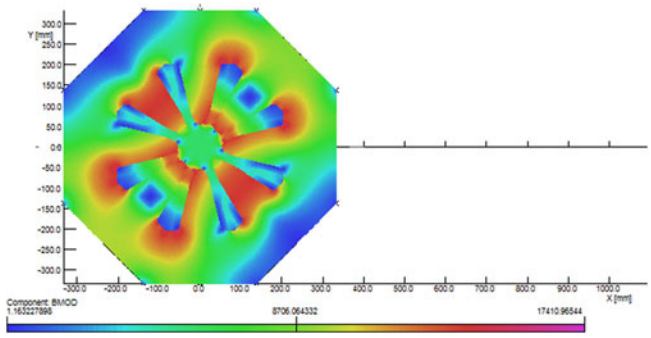

Fig. 3. The distribution of the flux density in the model at B = 5600 Gs.

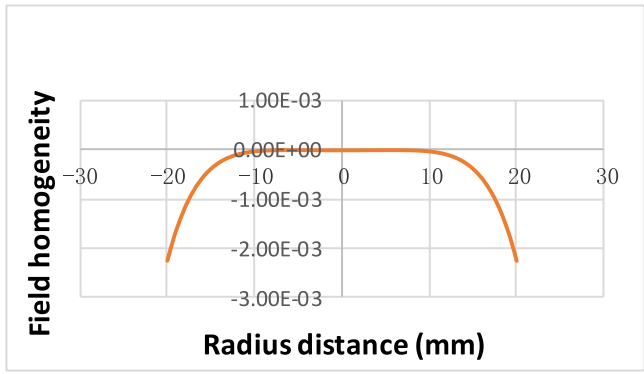

Fig. 4. Magnetic field homogeneity (ratio) within the good field region at the centry of the model.

of the pole. The 2D simulation result shows that when the field in the aperture reaches to 5600 Gs, the magnetic saturation occurs at the root of the pole. To decrease the flux density, we made the shape of the pole in a wedge to increase the cross section at the root of the pole. In addition, several chamfers were introduced to reduce the local saturation at the corners of the model. Fig. 3 shows the flux density distribution in the cross section of the model.

The optimization to improve the field quality in the good field region was also performed using Opera 2D. To achieve the required field homogeneity, we conducted extensive investigation on the pole shape optimization. Compared with flat surface, the octupole equipotential surface selected as the pole face can improve the field homogeneity in the aperture by 0.008. Besides, the tangent shims were introduced to compensate for multipole components at the edges of the poles. The length of the tangent shim is 1.239 mm. After these optimizations, the field homogeneity in the good field region of the magnet model is in the required range of $\pm 2.5 \times 10^{-3}$. The result of the field uniformity in the good field region is shown in Fig. 4.

B. 3D Static Simulation

The actual magnets are always assembled from steel laminations [6] and there are insulating layers between the steel laminations. The magnetic properties of the layer are different from the steel lamination, which makes magnet anisotropy. In the simulation, the effect of the anisotropy was taken into account by introducing a packing factor $f = 0.98$. The model of

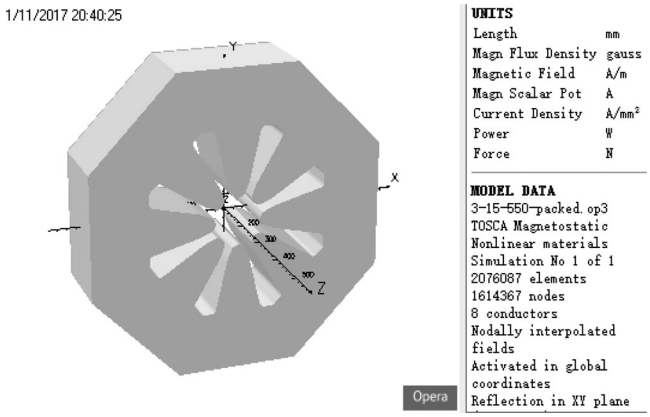

Fig. 5. The 3D model of the octupole scanning magnet for static simulation.

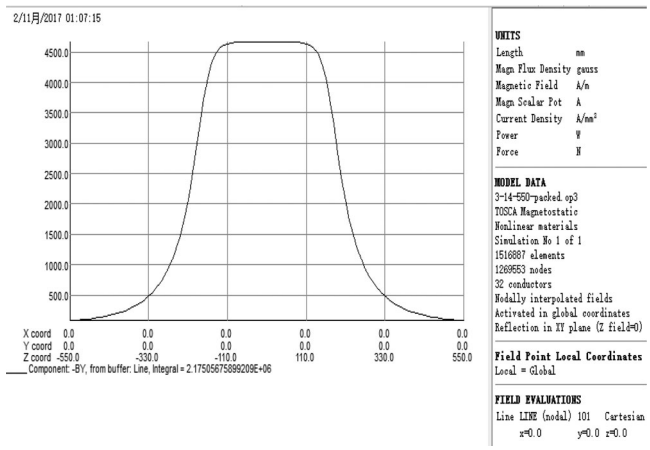

Fig. 6. The distribution of the magnetic field along z axis.

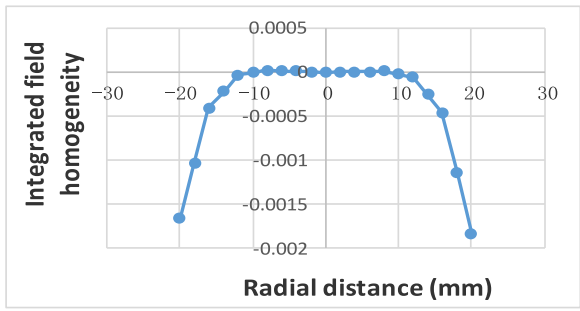

Fig. 7. The distribution of the integrated field homogeneity (ratio) along x axis.

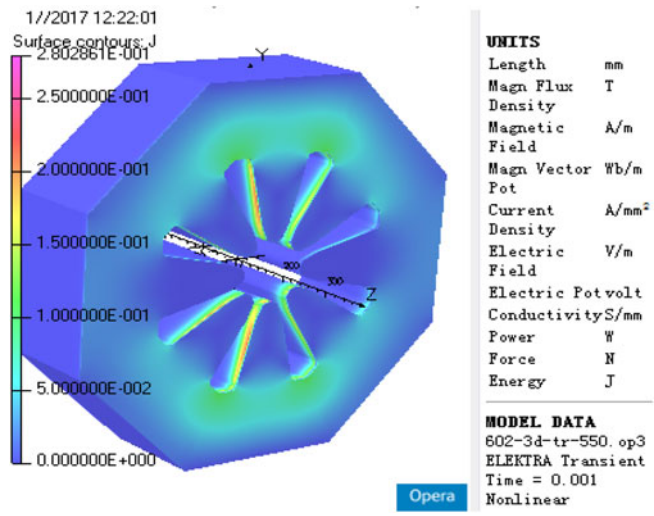

Fig. 8. The distribution of the eddy currents on the model at $t = 1$ ms.

the octupole scanning magnet was created in Opera 3D Modeller and solved using TOSCA solver. Fig. 5 shows the created model with a length of 350 mm. The distribution of the magnetic field along z axis is presented in Fig. 6. Although the maximum magnetic field is less than the required, the integrated field is 0.2175 Tm, which is larger than the assumed value. The corresponding deflection angle of the proton beam with an energy of 235 MeV is 92.530 mrad. As the center of the magnet model is 2.1m away from the iso-center, we obtain that the magnet deflects the beam by 19.43 cm. It indicates that the scanning area reaches the intended target. The integrated field homogeneity ($\delta = \int[\mathrm{B} - \mathrm{B}(0,0,\mathrm{z})]\mathrm{dz}/\int \mathrm{B}(0,0,\mathrm{z})\mathrm{dz}$) in the good field zone of the model was also calculated. The calculated result presented in Fig. 7 indicates that the integrated field homogeneity is within the range of $\pm 2.5 \times 10^{-3}$.

IV. 3D Time Dependent Simulation

A. Simulation of the Field Magnitude Varying With Time

The sinusoidal currents loaded on the four pairs of opposing poles must be with a same amplitude to generate a dipole magnetic field in the aperture of the model. The magnitude of the dipole magnetic field is proportional to the current amplitude. Besides related to the geometric position of the pole, the phase of the sinusoidal current loaded on the pole also changes with time. The magnitude of the phase change determines the deflection angle of the magnetic field, which is independent with current amplitude. The direction of the magnetic field varies, when the phase of the loaded sinusoidal current changes with time. Whether the magnetic field magnitude or direction changes with time, the eddy currents can be induced on the magnet model. In order to investigate the effect of the eddy currents on the magnetic field stability, some simulations were performed using Opera ELEKTRA.

We changed the magnitude of the sinusoidal currents to provide a field ramp of 0.3 ms from zero to 153.3 Gs for the model. Considering the anisotropy of the model, the conductivity was respectively set to 0 S/mm in the axial direction and 4000 S/mm in the plane perpendicular to the axial direction. The simulation was completed on a 2.4 GHz, 4 GB RAM computer and took 112 hours. Fig. 8 shows the distribution of the eddy currents on the magnet model at $\mathrm{t} = 1\mathrm{ms}$. It presents that the maximum eddy current density is 0.2803 A/mm^2.

The difference between the static and dynamic field is presented in Fig. 9. It indicates that the simulated dynamic field is approximately equal to the static field. The effect of the eddy currents on the stability of the field can be neglected after 1ms.

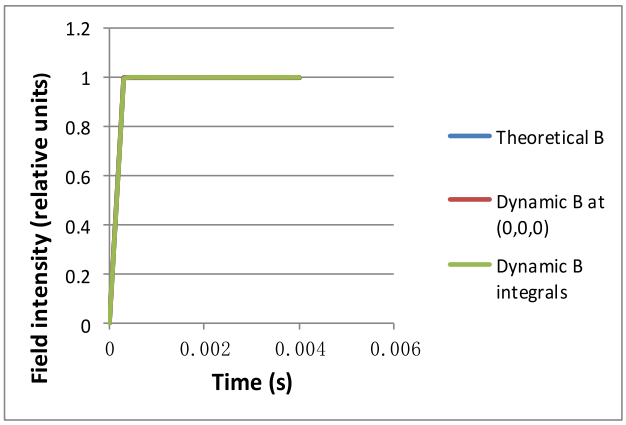

Fig. 9. Difference between static and dynamic field of the model. These multiple lines almost completely overlay each other, which indicates that the effect of the eddy current is negligible.

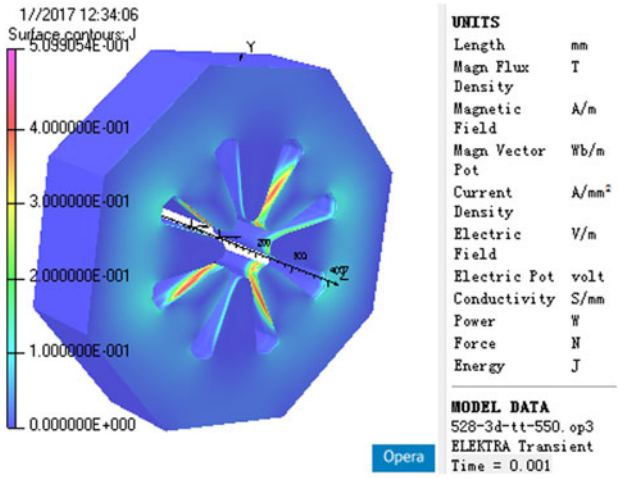

Fig. 10. The distribution of the eddy currents induced by the field rotation at $t = 1$ ms.

B. Simulation of the Magnetic Field Rotation

The simulation of the magnetic field rotation was also performed. The deflection angle of the field is equal to the magnitude of the phase change. The phases of the currents loaded on the four pairs of opposing poles must change synchronously to generate a rotating dipole magnetic field. In addition, the phases of the currents loaded a pair of opposing poles are always consistent. In the simulation, we change the phases of all currents loaded on the poles by 2° in 0.33 ms. In theory, the deflection angle of the field should also be 2° after 0.33 ms. Fig. 10 shows the distribution of the eddy currents on the model at $t = 1$ ms. The maximum eddy current density is 0.5099 A/mm^2.

The deflection angle of the field varying with time is presented in Fig. 11. The deflection angle of the field is 2.0003° at $t = 1$ ms. It indicates that the effect of the eddy currents on the field deflection is negligible.

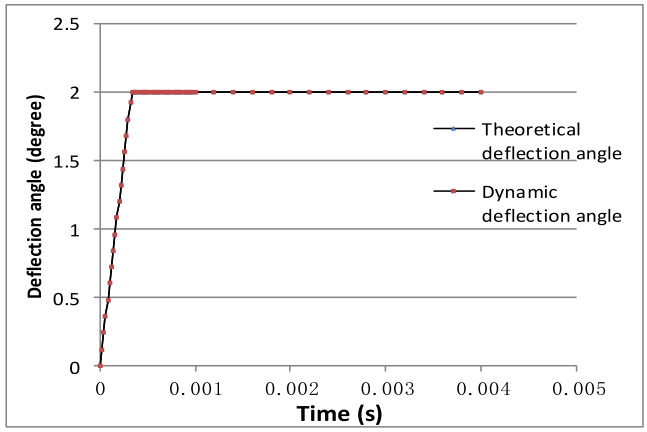

Fig. 11. The deflection angle of the magnetic field varying with time. The two lines almost overlay each other according to the simulation results.

V. Conclusion

The simulation results show that the radius of the good field region is approximately proportional to the aperture of the model in the required field uniformity. The introduction of the chamfers successfully reduced magnetic saturation at the corners of the model. The uniformity of the field integral was controlled below 2.5×10^{-3}. The integrated field reached 0.2175 Tm which was larger than the required. The effect of the eddy currents on the field stability was proved to be negligible and the stability time of the field was very short. All the simulation results including both static and dynamic indicate that the octupole scanning magnet can replace the two independent dipole magnets for spot scanning in proton therapy.

References

[1] V. Anferov, "Combined X–Y scanning magnet for conformal proton radiation therapy," *Med. Phys.*, vol. 32, no. 3, pp. 815–818, 2005.

[2] J. Gordon, P. Boisseau, A. Dart, and J. Flanz, "A multipole multipole magnet for pencil beam scanning," 2013. [Online]. Available: http://ptcusa.com/files/misc/P173%20A%20multipole%20magnet%20design%20for%20PBS.pdf.

[3] E. Pedroni, "Status of proton therapy: Results and future trends," in *Proc. 4th Eur. Particle Accelerator Conf.*, London, U.K., 1994, pp. 407–411.

[4] J. Gordon, R. P. Boisseau, and A. Dart, "System, apparatus and method for deflecting a particle beam," U.S. Patent 8378312 B1, 2013.

[5] W. Chu *et al.*, "Performance specifications for proton medical facility," Lawrence Berkeley Lab., Berkeley, CA, USA, Tech. Rep. LBL-33749, 1993.

[6] S. Das, V. Thakur, R. Mishra, and G. Singh, "Design of new dipole magnet for the exiting booster synchrotron at RRCAT," in *Proc. DAE-BRNS Indian Particle Accelerator Conf.*, 2009, Paper no. 238.